



Massive Unsourced Random Access Under Carrier Frequency Offset

XIE Xinyu¹, WU Yongpeng¹, YUAN Zhifeng^{2,3}, MA Yihua^{2,3}

(1. Shanghai Jiao Tong University, Shanghai 200240, China;

2. ZTE Corporation, Shenzhen 518057, China;

3. State Key Laboratory of Mobile Network and Mobile Multimedia Technology, Shenzhen 518055, China)

DOI: 10.12142/ZTECOM.202303007

<https://link.cnki.net/urlid/34.1294.TN.20230830.1507.003>, published online August 30, 2023

Manuscript received: 2022-05-22

Abstract: Unsourced random access (URA) is a new perspective of massive access which aims at supporting numerous machine-type users. With the appearance of carrier frequency offset (CFO), joint activity detection and channel estimation, which is vital for multiple-input and multiple-output URA, is a challenging task. To handle the phase corruption of channel measurements under CFO, a novel compressed sensing algorithm is proposed, leveraging the parametric bilinear generalized approximate message passing framework with a Markov chain support model that captures the block sparsity structure of the considered angular domain channel. An uncoupled transmission scheme is proposed to reduce system complexity, where slot-emitted messages are reorganized relying on clustering unique user channels. Simulation results reveal that the proposed transmission design for URA under CFO outperforms other potential methods.

Keywords: activity detection; channel estimation; frequency offset; massive machine-type communication; massive MIMO

Citation (Format 1): XIE X Y, WU Y P, YUAN Z F, et al. Massive unsourced random access under carrier frequency offset [J]. *ZTE Communications*, 2023, 21(3): 45 – 53. DOI: 10.12142/ZTECOM.202303007

Citation (Format 2): X. Y. Xie, Y. P. Wu, Z. F. Yuan, et al., “Massive unsourced random access under carrier frequency offset,” *ZTE Communications*, vol. 21, no. 3, pp. 45 – 53, Sept. 2023. doi: 10.12142/ZTECOM.202303007.

1 Introduction

Massive machine-type communication (mMTC)^[1], also known as massive access^[2], is one of the three typical application scenarios in the 5G mobile communication system. mMTC aims at establishing reliable communications for a massive number of cheap devices with sporadic data stream patterns and short packet length, which is quite different from conventional human-type communications (HTC). Hence, the design of efficient massive connectivity schemes requires investigating novel theories and paradigms.

To reduce signaling overhead and latency, existing mMTC schemes generally follow a grant-free random access (RA) protocol^[3] where users directly transmit data to the base station (BS) without any approval. One type of grant-free RA scheme^[4-6] allocates unique pilots as identities to users; they are sent first as preambles for activity detection (AD) and channel estimation (CE). Data transmission happens in the next stage leveraging efficient RA techniques like sparse code multiple access (SCMA)^[7] with individual user codebooks. A novel paradigm of unsourced random access (URA) was first

addressed in Ref. [8]. Different from pilot-based RA schemes, URA users are forced to use the same codebook for data transmission. Since the transmitted codewords contain no user identities, the BS only acquires a list of transmitted messages without linking them to specific active users. A finite block-length (FBL) achievability bound was derived in Ref. [8], and it is found that there exists an important gap between conventional RA schemes like ALOHA and the benchmark.

It is evident that an intuitive URA scheme is closely related to a compressed sensing (CS) recovery problem, involving AD to the set of codewords each linked to a potential message sequence. However, directly applying CS techniques is impractical because the codebook size grows exponentially to the message length. To approach the FBL bound with manageable complexity, the coded compressed sensing (CCS) framework^[9] is investigated which couples an outer tree code and an inner CS code. More specifically, each datum is partitioned into several sub-blocks; they are coupled by appending parity check bits generated from linear block coding, thereby forming fragments to be sent over multiple slots using a common codebook. The BS detects codeword activity via a CS recovery method, and then reconstructs the original messages by a tree-based forward error correction strategy.

Utilizing a large number of antennas at the BS, the massive

This work was supported by the ZTE Industry-University-Institute Cooperation Funds under Grant No. HC-CN-20201116001.

multiple-input and multiple-output (MIMO) technology provides high spatial resolution within the same time/frequency resource to increase spectral efficiency. Different from additive white Gaussian noise (AWGN) channels, it requires channel estimation for detection under MIMO fading channels, forming URA a joint AD and CE (JADCE) problem that is considered as a multiple measurement vector (MMV) problem and solved by CS algorithms like approximate message passing (AMP)^[4]. Leveraging channel structural sparsity in the virtual angular domain, Ref. [5] presented a performance gain by performing AD at the spatial domain and CE at the angular domain. Promoting the CCS-based URA to the massive MIMO scenario, the work of Ref. [10] introduced a covariance-based paradigm and proposed a maximum likelihood decoder estimating large-scale fading coefficients (LSFCs) for AD. Ref. [11] further promoted the case of independent and identically distributed (i.i.d.) channels considered in Ref. [10] to the case of correlated channels. Leveraging the rich spatial information reserved in multiple antennas, Refs. [12 – 14] captured the strong similarity/correlation between slot-wise user channels and proposed uncoupled URA transmission schemes. In Refs. [13] and [14], the authors considered the angular domain MIMO channel and proposed an expectation-maximization-aided generalized approximate message passing algorithm with a Markov random field support structure (EM-MRF-GAMP) for JADCE. The similar statistics of slot-wise channels of each user couple the split message fragments, which eliminates the need for redundancies to improve the coding rate. Accordingly, message stitching takes on the form of a clustering decoder, recognizing slot-distributed channels of each active user based on similarity. Eliminating the need for redundancies in CCS, the uncoupled URA schemes^[12–14] achieve higher coding rates and spectral efficiency.

Unfortunately, all the above works consider an ideal scenario where users are perfectly synchronized with the BS. However, caused by the mismatch between the carrier frequencies of the local oscillators at users and the BS, carrier frequency offset (CFO) inevitably exists. CFO corrupts the phase of channel measurements and imposes significant contamination on the JADCE results. Few works in the context of massive access address the issue of CFO estimation. In Ref. [15], the authors adopted a Lasso-based method for CFO estimation, but only focused on the AD results. The authors of Ref. [16] introduced a CS method for JADCE under CFO in the framework of orthogonal frequency division multiple access (OFDMA). The key idea is to expand the measurement matrix with a finite number of discrete frequency offsets sampled in the possible region. The JADCE problem as a generalized MMV problem with structured sparsity is then solved by the proposed structured-GAMP algorithm. However, the CFO estimation in Ref. [16] is discrete, and the measurement matrix size will increase accordingly in URA applications, resulting in greater computational complexity. To our knowledge, no ex-

isting work has discussed URA under CFO.

In this paper, confronted with the issue of CFO, we formulate URA as a JADCE problem with a bilinear signal detection structure. We consider the MIMO channel in the angular domain to promote the sparsity of the CS problem. A novel CS algorithm termed Markov-chain-aided parametric bilinear generalized approximate message passing (MC-PBiGAMP) is proposed for JADCE, which captures the clustered sparsity structure of the angular domain channel. An uncoupled transmission design for URA is then employed to reduce system complexity. With messages divided for slotted emitting, data list reconstruction is conducted in the form of a clustering decoder leveraging unique channel statistics. Simulation results show that the proposed method outperforms state-of-the-art approaches in terms of JADCE and reaches reliable URA system performance.

The rest of the paper is organized as follows. The URA system model is given in the next section. In Section 3, the MC-PBiGAMP algorithm is proposed for JADCE under CFO. Then, the uncoupled URA transmission design of low complexity is discussed in Section 4. Numerical results are presented in Section 5, followed by concluding remarks drawn in Section 6. Throughout this paper, the j -th column and i -th row of matrix \mathbf{X} are denoted by \mathbf{x}_j and $\mathbf{x}_{i,:}$, respectively, and the (i,j) -th entry of \mathbf{X} is represented by $x_{i,j}$; $(\cdot)^T$, $(\cdot)^*$, and $(\cdot)^H$ stand for the conjugate, transpose, and conjugate transpose, respectively. Denote $\|\mathbf{x}\|$ the Euclid norm of vector \mathbf{x} , and $\|\cdot\|_2$ and $\|\cdot\|_F$ represent the the l_2 -norm and the Frobenius norm, respectively. For an integer $X > 0$, the shorthand notation $[X]$ stands for the set $\{1, 2, \dots, X\}$. Finally, $\mathcal{CN}(x; \hat{x}, \mu^x)$ signifies the complex Gaussian distribution of a random variable x with mean \hat{x} and variance μ^x .

2 System Model

In this paper, we consider an uplink transmission scenario where K_a active users communicate to a single BS equipped with a uniform linear array (ULA) of M half-wavelength spaced antennas. The channel $\tilde{\mathbf{h}}_k \in \mathbb{C}^M$ between the k -th user and the BS is described on a geometric basis as^[5]

$$\tilde{\mathbf{h}}_k = \sqrt{\rho_k} \sum_{l=1}^L \mathbf{g}_{k,l} \mathbf{e}(\theta_{k,l}), \quad (1)$$

where ρ_k is the LSFC which follows the standard Log-distance path loss model as $\log_{10} \rho_k = -128.1 - 37.6 \log_{10}(D_k)$ with distance D_k measured in km, $\mathbf{g}_{k,l} \sim \mathcal{CN}(0, 1)$ is the complex path gain of the l -th path, $\theta_{k,l} \in [-\pi/2, \pi/2]$ is the angle of arrival (AOA), and $\mathbf{e}(\theta_{k,l})$ is given by

$$\mathbf{e}(\theta_{k,l}) = \frac{1}{\sqrt{M}} \left[1, e^{-j\pi \sin \theta_{k,l}}, \dots, e^{-j\pi(M-1) \sin \theta_{k,l}} \right]^T. \quad (2)$$

The spatial domain channel can be transformed to the angu-

lar domain by

$$\mathbf{h}_k = \mathbf{U}_M^H \tilde{\mathbf{h}}_k, \quad (3)$$

where \mathbf{U}_M^H is the M -dimensional discrete Fourier transform (DFT) matrix. The angular domain channel is sparse with few elements of dominant magnitude. This is attributed to the high spatial resolution of massive MIMO, leveraging large-scale antennas against finite propagation paths. Also, due to the spectral leakage of DFT, the angular domain channel reveals a clustered sparsity structure with nonzero elements spaced adjacent to dominant elements^[17].

In the URA scenario, active users pick up codewords/columns from a common codebook/coding matrix to transmit the B -bit payload. We choose to generate the common codebook by the sparse regression code^[18]. Each entry of the codebook $\mathbf{A} = [\mathbf{a}_1, \dots, \mathbf{a}_{2^B}] \in \mathbb{C}^{N \times 2^B}$ is generated from an i.i.d. Gaussian distribution $\mathcal{CN}(1, 1/N)$ such that $\mathbb{E}\{\|\mathbf{a}\|_2^2\} = 1$. We assume that oscillators at users are synchronized to the same frequency through calibration^[19-20], i.e., CFOs are the same for all users. Considering a block fading channel where channel coefficients remain unchanged in N symbol transmissions, the received signal at the BS under CFO is represented as

$$\tilde{\mathbf{Y}} = \sum_k \text{diag}(\boldsymbol{\tau}(\omega)) \mathbf{a}_i \tilde{\mathbf{h}}_k^T + \tilde{\mathbf{W}} = \text{diag}(\boldsymbol{\tau}(\omega)) \mathbf{A} \tilde{\mathbf{H}} + \tilde{\mathbf{W}}, \quad (4)$$

where $\omega \triangleq 2\pi\Delta f T$ with Δf the frequency offset between users and the BS in Hz and T the sampling period, $\boldsymbol{\tau}(\omega) = [1, e^{j\omega}, \dots, e^{j(N-1)\omega}]^T$ is the corresponding phase rotation vector due to CFO, $\mathbf{B} \in \{0, 1\}^{2^B \times K_s}$ is a selection matrix, $\tilde{\mathbf{H}} = [\tilde{\mathbf{h}}_1, \dots, \tilde{\mathbf{h}}_{K_s}]^T \in \mathbb{C}^{K_s \times M}$, and $\tilde{\mathbf{W}}$ is the AWGN matrix with elements generated from i.i.d. $\mathcal{CN}(0, \sigma_w^2)$. The (i, k) -th entry of \mathbf{B} is nonzero only if the k -th user transmits the information sequence \mathbf{m}_k with $\text{decimal}(\mathbf{m}_k) = i$, where $\text{decimal}(\mathbf{m}_k)$ is the the radix ten equivalent of \mathbf{m}_k . The received signal in the angular domain can be calculated as

$$\mathbf{Y} = \text{diag}(\boldsymbol{\tau}(\omega)) \mathbf{A} \tilde{\mathbf{H}} \mathbf{U}_M^* + \tilde{\mathbf{W}} \mathbf{U}_M^* = \text{diag}(\boldsymbol{\tau}(\omega)) \mathbf{A} \mathbf{B} \mathbf{H} + \mathbf{W}, \quad (5)$$

where $\mathbf{H} = [\mathbf{h}_1, \dots, \mathbf{h}_{K_s}]^T$, and $\mathbf{W} \triangleq \tilde{\mathbf{W}} \mathbf{U}_M^*$ is the equivalent noise matrix.

3 Proposed Algorithm for JADCE under CFO

3.1 Problem Formulation and Probability Model

Data detection in URA is to determine which column of \mathbf{A} is transmitted. For better illustration, we rewrite Eq. (5) as

$$\mathbf{Y} = \text{diag}(\mathbf{U}_N^* \mathbf{c}) \mathbf{A} \mathbf{X} + \mathbf{W} = \mathbf{Z} + \mathbf{W}, \quad (6)$$

where \mathbf{U}_N is the N -dimensional DFT matrix, $\mathbf{c} = \mathbf{U}_N^T \boldsymbol{\tau}(\omega)$ is

sparse due to the Vandermonde structure of $\boldsymbol{\tau}(\omega)$, $\mathbf{X} \triangleq \mathbf{B} \mathbf{H}$, and $\mathbf{Z} \triangleq \text{diag}(\mathbf{U}_N^* \mathbf{c}) \mathbf{A} \mathbf{X}$. Since $K_s \ll 2^B$, \mathbf{X} is row sparse. Furthermore, the sparse rate of \mathbf{X} is promoted due to the sparsity of angular domain channels. Our purpose is to recover sparse \mathbf{c} and \mathbf{X} from the noisy observation \mathbf{Y} with known \mathbf{U}_N and \mathbf{A} , recognized as a CS recovery problem. Note that the URA receiver does not attempt to link the message to its source device, therefore, we do not need to reconstruct \mathbf{B} .

To solve the structured-matrix estimation problem, we start with reformulating the random variable dependency corresponding to Eq. (6), taking on the form

$$z_{n,m} = \sum_{i=1}^N \sum_{j=1}^{2^B} c_i z_{n,m}^{(i,j)} x_{j,m}, \quad (7)$$

where $z_{n,m}^{(i,j)} \triangleq u_{n,i} a_{n,j}$ is an element of a third-order tensor $\{\mathbf{z}_n^{(i,j)} = [z_{n,1}^{(i,j)}, \dots, z_{n,M}^{(i,j)}]^T\}_{i,j}$. For the sparse vector \mathbf{c} , we assign a Bernoulli-Gaussian prior to each independent component c_i , i.e.,

$$p(c_i) = \lambda_c \delta(c_n) + (1 - \lambda_c) \mathcal{CN}(0, \sigma_c^2), \quad (8)$$

where λ_c is the sparsity fraction of \mathbf{c} and $\delta(\cdot)$ represents the Dirac-delta function. Similarly, a Bernoulli-Gaussian prior is used to model the conditional probability

$$p(x_{j,m} | s_{j,m}) = \delta(x_{j,m}) \delta(s_{j,m} + 1) + \mathcal{CN}(x_{j,m}; 0, \sigma_x^2) \delta(s_{j,m} - 1), \quad (9)$$

where $s_{j,m} \in \{-1, 1\}$ is the binary state of $x_{j,m}$ with $s_{j,m} = \pm 1$ signifying that $x_{j,m}$ is nonzero/zero. To capture the clustered sparsity of the angular domain channel support $\mathbf{s}_{j,:} = [s_{j,1}, \dots, s_{j,M}]$, we employ the Markov chain (MC) model^[21] as follows

$$p(\mathbf{s}_{j,:}) = p(s_{j,1}) \prod_{m=2}^M p(s_{j,m} | s_{j,m-1}), \quad (10)$$

where the transition probability $p(s_{j,m} | s_{j,m-1})$ is given by

$$p(s_{j,m} | s_{j,m-1}) = \begin{cases} (1 - p_{01})^{1-s_{j,m}} p_{01}^{s_{j,m}}, & s_{j,m-1} = 0 \\ (1 - p_{10})^{s_{j,m}} p_{10}^{1-s_{j,m}}, & s_{j,m-1} = 1 \end{cases}, \quad (11)$$

and $p(s_{j,1})$ is initialized as a steady-state distribution with $p(s_{j,1} = 0) = p_{10}/(p_{01} + p_{10})$ and $p(s_{j,1} = 1) = p_{10}/(p_{01} + p_{10})$. The MC model depicts the average cluster size and the average gap between two clusters by parameters p_{10} and p_{01} , respectively. A smaller value of p_{10} indicates a larger cluster length and a smaller value of p_{01} leads to a larger average gap between two clusters. And in general, the sparsity of \mathbf{x} is measured as $\lambda_x \triangleq p_{10}/(p_{01} + p_{10})$.

Following the Bayesian theory, we derive the posterior probability density of \mathbf{c} and \mathbf{X} given \mathbf{Y} as

$$p(\mathbf{c}, \mathbf{X} | \mathbf{Y}) \propto \prod_{n,m} p(y_{n,m} | z_{n,m}) \prod_i p(c_i) \prod_j p(\mathbf{x}_{j,m} | s_{j,m}) p(s_{j,m}). \quad (12)$$

The variable dependencies are shown in a factor graph in Fig. 1. Performing the minimum mean square error (MMSE) or maximum a posteriori (MAP) estimation of Eq. (12) is impractical since it comes down to marginalizing a joint distribution with high dimensions. Therefore, we use an approximate message passing approach that is detailed in Section 3.2.

3.2 Approximate Message Passing Algorithm for Signal Reconstruction

PBiGAMP^[22] employs loopy belief propagation (BP) over the factor graph to make approximate inferences of the marginal. According to the sum-product rule and the central limit theorem (CLT), messages passed between the edges of the factor graph possess Gaussian approximations under the large system limit assumption (i.e., $2^B \rightarrow \infty$). Message-passing component updates are given in Algorithm 1.

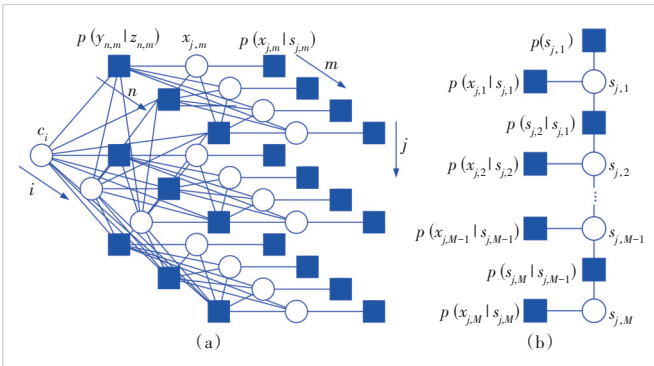
Algorithm 1. MC-PBiGAMP for JADCE under CFO

Input: $\mathbf{Y}, \mathbf{A}, U_N, T_{\max}, T_{\text{mc}}, \tau$

Initialize: $\forall n, m: \hat{s}_{n,m}(0) = 0, \forall i, j, m: \text{choose } \hat{x}_{j,m}(1), \mu_{j,m}^x(1), \hat{c}_i(1), \mu_i^c(1)$

for $t = 1, \dots, T_{\max}$ **do**

$$\begin{aligned} \forall n, m, i: \hat{z}_{n,m}^{(i,*)}(t) &= \sum_{j=1}^{2^B} z_{n,m}^{(i,j)} \hat{x}_{j,m}(t) \\ \forall n, m, j: \hat{z}_{n,m}^{(*,j)}(t) &= \sum_{i=1}^N \hat{c}_i(t) z_{n,m}^{(i,j)} \\ \forall n, m: \hat{z}_{n,m}^{(*,*)}(t) &= \sum_{i=1}^N \hat{c}_i(t) \hat{z}_{n,m}^{(i,*)}(t) = \sum_{j=1}^{2^B} \hat{z}_{n,m}^{(*,j)}(t) \hat{x}_{j,m}(t) \\ \bar{\mu}_{n,m}^p(t) &= \sum_{i=1}^N \mu_i^c(t) \left| \hat{z}_{n,m}^{(i,*)}(t) \right|^2 + \sum_{j=1}^{2^B} \mu_{j,m}^x(t) \left| \hat{z}_{n,m}^{(*,j)}(t) \right|^2 \\ \mu_{n,m}^p(t) &= \bar{\mu}_{n,m}^p(t) + \sum_{i=1}^N \mu_i^c(t) \sum_{j=1}^{2^B} \mu_{j,m}^x(t) \left| z_{n,m}^{(i,j)} \right|^2 \\ \hat{p}_{n,m}(t) &= \hat{z}_{n,m}^{(*,*)}(t) - \hat{s}_{n,m}(t-1) \bar{\mu}_{n,m}^p(t) \\ \mu_{n,m}^z(t) &= \text{Var} \left\{ z_{n,m} | \mathbf{Y}; \hat{p}_{n,m}(t), \mu_{n,m}^p(t), \sigma_w \right\} \\ \hat{z}_{n,m}(t) &= \mathbb{E} \left\{ z_{n,m} | \mathbf{Y}; \hat{p}_{n,m}(t), \mu_{n,m}^p(t), \sigma_w \right\} \end{aligned}$$



▲ Figure 1. Factor graph for Bayesian inference

$$\begin{aligned} \mu_{n,m}^s(t) &= (1 - \mu_{n,m}^z(t) / \mu_{n,m}^p(t)) / \mu_{n,m}^p(t) \\ \hat{s}_{n,m}(t) &= (\hat{z}_{n,m}(t) - \hat{p}_{n,m}(t)) / \mu_{n,m}^p(t) \\ \forall j, m: \mu_{j,m}^r(t) &= \left(\sum_{n=1}^N \mu_{n,m}^s(t) \left| \hat{z}_{n,m}^{(*,j)}(t) \right|^2 \right)^{-1} - \\ &\quad \mu_{j,m}^r(t) \hat{x}_{j,m}(t) \sum_{n=1}^N \mu_{n,m}^s(t) \sum_{i=1}^N \mu_i^c(t) \left| z_{n,m}^{(i,j)} \right|^2 \\ \forall i: \mu_i^q(t) &= \left(\sum_{n=1}^N \mu_{n,m}^s(t) \left| \hat{z}_{n,m}^{(i,*)}(t) \right|^2 \right)^{-1} - \\ &\quad \mu_i^q(t) \hat{c}_i(t) \sum_{n=1}^N \sum_{m=1}^M \mu_{n,m}^s(t) \sum_{j=1}^{2^B} \mu_{j,m}^x(t) \left| z_{n,m}^{(i,j)} \right|^2 \\ \forall j, m: \mu_{j,m}^x(t+1) &= \text{Var} \left\{ x_{j,m} | \mathbf{Y}; \hat{r}_{j,m}(t), \mu_{j,m}^r(t), \bar{\rho}_{j,m}(t), \sigma_x \right\} \\ \hat{x}_{j,m}(t+1) &= \mathbb{E} \left\{ x_{j,m} | \mathbf{Y}; \hat{r}_{j,m}(t), \mu_{j,m}^r(t), \bar{\rho}_{j,m}(t), \sigma_x \right\} \\ \forall i: \mu_i^c(t+1) &= \text{Var} \left\{ c_i | \mathbf{Y}; \hat{q}_i(t), \mu_i^q(t), \lambda_c, \sigma_c \right\} \\ \hat{c}_i(t+1) &= \mathbb{E} \left\{ c_i | \mathbf{Y}; \hat{q}_i(t), \mu_i^q(t), \lambda_c, \sigma_c \right\} \\ \text{if } \left\| \hat{Z}^{(*,*)}(t) - \hat{Z}^{(*,*)}(t-1) \right\|_F^2 &\leq \tau \left\| \hat{Z}^{(*,*)}(t) \right\|_F^2, \text{ stop} \\ \text{end for} \\ \text{Output: } \hat{\mathbf{c}} &= \hat{\mathbf{c}}(t), \hat{\mathbf{X}} = \hat{\mathbf{X}}(t) \end{aligned}$$

The reader can refer to Ref. [22] for detailed derivations. Briefly, the calculation of messages from all variable nodes $\{c_i\}_{\forall i}$ and $\{x_{j,m}\}_{\forall j,m}$ to factor node $p(y_{n,m}|z_{n,m})$ takes on the form of a complex Gaussian distribution $\mathcal{CN}(z_{n,m}; \hat{p}_{n,m}, \mu_{n,m}^p)$. With $p(y_{n,m}|z_{n,m}) = \exp(-\|y_{n,m} - z_{n,m}\|^2 / \sigma_w^2) / \pi \sigma_w^2$ under AWGN, the marginal posterior $p(z_{n,m} | \mathbf{Y})$ is inferred as

$$p(z_{n,m} | \mathbf{Y}; \hat{p}_{n,m}, \mu_{n,m}^p, \sigma_w) = \mathcal{CN}(z_{n,m}; \hat{z}_{n,m}, \mu_{n,m}^z), \quad (13)$$

with

$$\hat{z}_{n,m} = \frac{\mu_{n,m}^p y_{n,m} + \sigma_w^2 \hat{p}_{n,m}}{\mu_{n,m}^p + \sigma_w^2}, \quad (14)$$

$$\mu_{n,m}^z = \frac{\mu_{n,m}^p \sigma_w^2}{\mu_{n,m}^p + \sigma_w^2}, \quad (15)$$

where $\hat{s}_{n,m}$ and $\mu_{n,m}^s$ are the scaled residual and the residual variance, respectively. Again, the message from factor node $p(y_{n,m}|z_{n,m})$ to variable node c_i is approximately Gaussian ($\mathcal{CN}(c_i; \hat{q}_i, \mu_i^q)$). We reach the estimation of the posterior mean and variance of $p(c_i | \mathbf{Y})$ as

$$\hat{c}_i = \mathbb{E} \left\{ c_i | \mathbf{Y}; \hat{q}_i, \mu_i^q, \lambda_c, \sigma_c \right\} = \lambda_c \frac{\hat{q}_i \sigma_c^2}{\mu_i^q + \sigma_c^2}, \quad (16)$$

$$\mu_i^c = \text{Var} \left\{ c_i | \mathbf{Y}; \hat{q}_i, \mu_i^q, \lambda_c, \sigma_c \right\} = \lambda_c \frac{\mu_i^q \sigma_c^2}{\mu_i^q + \sigma_c^2} + \lambda_c (1 - \lambda_c) \left| \hat{c}_i \right|^2. \quad (17)$$

As for messages passed within the MC model, the input, i.e., the message from variable node $x_{j,m}$ to factor node $p(x_{j,m}|s_{j,m})$ is a complex Gaussian distribution with mean $\hat{r}_{j,m}$ and variance $\mu_{j,m}^r$. Then, we have the message from factor node $p(x_{j,m}|s_{j,m})$ to variable node $s_{j,m}$ computed as

$$\vec{v}_{j,m} = \vec{\rho}_{j,m} \delta(s_{j,m} - 1) + (1 - \vec{\rho}_{j,m}) \delta(s_{j,m} + 1), \quad (18)$$

where

$$\vec{\rho}_{j,m} = \left(1 + \frac{\mathcal{CN}(0; \hat{r}_{j,m}, \mu_{j,m}^r)}{\int_{x_{j,m}} \mathcal{CN}(x_{j,m}; 0, \sigma_x^2) \mathcal{CN}(x_{j,m}; \hat{r}_{j,m}, \mu_{j,m}^r)} \right)^{-1}. \quad (19)$$

The forward message passing over MC $s_{j,i}$ is conducted in a recursive way as follows^[21]

$$\vec{\varphi}_{j,1} = \lambda_x = \frac{p_{01}}{p_{01} + p_{10}}, \quad (20)$$

$$\vec{\varphi}_{j,m} = \frac{p_{01}(1 - \vec{\rho}_{j,m-1})(1 - \vec{\varphi}_{j,m-1}) + p_{11}\vec{\rho}_{j,m-1}\vec{\varphi}_{j,m-1}}{(1 - \vec{\rho}_{j,m-1})(1 - \vec{\varphi}_{j,m-1}) + \vec{\rho}_{j,m-1}\vec{\varphi}_{j,m-1}}. \quad (21)$$

The backward message passing is performed in a similar way^[21]:

$$\vec{\varphi}_{j,M} = \frac{1}{2}, \quad (22)$$

$$\vec{\varphi}_{j,m} = \frac{p_{10}(1 - \vec{\rho}_{j,m+1})(1 - \vec{\varphi}_{j,m+1}) + (1 - p_{10})\vec{\rho}_{j,m+1}\vec{\varphi}_{j,m+1}}{(p_{00} + p_{10})(1 - \vec{\rho}_{j,m+1})(1 - \vec{\varphi}_{j,m+1}) + (p_{11} + p_{01})\vec{\rho}_{j,m+1}\vec{\varphi}_{j,m+1}}. \quad (23)$$

Subsequently, the message from variable node $s_{j,m}$ to factor node $p(x_{j,m}|s_{j,m})$ is represented as

$$\vec{v}_{j,m} = \vec{\rho}_{j,m} \delta(s_{j,m} - 1) + (1 - \vec{\rho}_{j,m}) \delta(s_{j,m} + 1), \quad (24)$$

where

$$\vec{\rho}_{j,m} = \frac{\vec{\varphi}_{j,m} \vec{\varphi}_{j,m}}{(1 - \vec{\varphi}_{j,m})(1 - \vec{\varphi}_{j,m}) + \vec{\varphi}_{j,m} \vec{\varphi}_{j,m}}. \quad (25)$$

After that, the output of the MC support estimation module, i.e., the message from factor node $p(x_{j,m}|s_{j,m})$ to variable node $x_{j,m}$ is expressed as a Bernoulli-Gaussian distribution $\vec{\rho}_{j,m} \mathcal{CN}(x_{j,m}; 0, \sigma_x^2) + (1 - \vec{\rho}_{j,m}) \delta(x_{j,m})$. Finally, we calculate the posterior mean and variance of $p(x_{j,m}|\mathbf{Y})$ as^[13]

$$\hat{x}_{j,m} = \mathbb{E}\{x_{j,m}|\mathbf{Y}; \hat{r}_{j,m}, \mu_{j,m}^r, \vec{\rho}_{j,m}, \sigma_x\} = \vec{\rho}_{j,m} \frac{\hat{r}_{j,m} \sigma_x^2}{\mu_{j,m}^r + \sigma_x^2}, \quad (26)$$

$$\mu_{j,m}^x = \vec{\rho}_{j,m} \frac{\mu_{j,m}^r \sigma_x^2}{\mu_{j,m}^r + \sigma_x^2} + \vec{\rho}_{j,m} (1 - \vec{\rho}_{j,m}) |\hat{x}_{j,m}|^2. \quad (27)$$

The above message components are updated iteratively until a certain stopping criterion is satisfied. The worst-case complexity order of the proposed algorithm per iteration is $\mathcal{O}(2^B N^2 M)$. With \hat{X} (the estimation of X), the active codebooks are determined as

$$X = \left\{ j: \|\hat{x}_j\|^2 > \phi, j \in [2^B] \right\}, \quad (28)$$

where $\phi > 0$ is the threshold.

4 Uncoupled URA Transmission Scheme for Complexity Reduction

Since the size of common codebook A grows exponentially in B , it is computationally infeasible for any CS algorithm to perform AD among the codebook accommodating even small-sized messages (e.g., $B = 100$ bit). Many URA works take the divide-and-conquer strategy and utilize a concatenated coding scheme termed CCS. Specifically, each long message bit sequence is split into several fragments of amenable length for slotted transmission. These fragments are coupled by appending parity check bits generated by pseudo-random linear combinations of message bits from previous fragments. The decoder first determines transmitted fragments of each slot and then combines slot-wise fragments into the entire message based on a tree decoding process. With the help of the high spatial resolution provided by massive MIMO, it is suggested in Refs. [13] and [14] that the massive MIMO channels in the angular domain already offer adequate information to combine fragments scattered among different transmission slots. The sparsity and magnitude of each entry of angular domain channel vectors indicate angular propagation patterns unique to each active user. Assuming these channel statistics to be almost unchanged within the URA uplink transmission period, the message stitching process can be conducted in the form of clustering recovered channels into groups of each active user.

Following the uncoupled URA scheme in Refs. [13] and [14], we divide each B -bit message into S fragments of length $J = B/S$, which are encoded for transmission in the coherent block of length $N = N_s S$. The designed low-complexity URA receiver under CFO in this paper reconstructs the emitted message list by taking the following two steps: 1) after each transmission slot, performing JADCE to the received signal via the proposed MC-PBiGAMP algorithm with downsized common coding matrix $\tilde{A} \in \mathbb{C}^{N_s \times 2^J}$; 2) reconstructing the en-

tire message sequence by combining slot-wise codewords according to the similarity of their corresponding channels. In the rest of the section, we discuss the slot-balanced K -means algorithm designed for message stitching.

4.1 Slot-Balanced K -Means for Clustering-Based Message Stitching

We consider an ideal case where no users transmit identical data in the same transmission slot. Therefore, K_a codewords are exactly judged to be active in every slot. The purpose of the decoder is to classify active codewords into K_a groups based on the similarity of their corresponding channel vectors. During the clustering process, two obvious constraints must be satisfied: 1) Channels from the same slot cannot be assigned to the same group; 2) each group must be composed of S channels at the end of the clustering.

Slot-balanced K -means algorithm^[14] is tailored for the application scenario, performing assignment steps on a per-slot basis and obtaining groups with identical numbers of components. To meet Constraint 2 in K -means, the assignment step is performed slot by slot, i. e., all K_a active channels recognized in the same slot are simultaneously allocated to K_a groups. Then, the assignment problem with Constraint 1 is equivalent to the minimum bipartite matching problem, which can be well solved by the Hungarian algorithm^[23]. We define $\mathbf{g}_k^s \in \mathbb{C}^M$ the k -th active channel vector at the s -th slot, $\mathbf{c}_{k'} \in \mathbb{C}^M$ the k' -th group center, and $\mathbf{C} = [\mathbf{c}_1, \dots, \mathbf{c}_{K_s}]$. The input $\mathbf{D} \in \mathbb{C}^{K_a \times K_a}$ of the Hungarian algorithm is calculated as each element $d_{k,k'} = \|\mathbf{g}_k - \mathbf{c}_{k'}\|_2$. The output of the algorithm is a binary matrix $\mathbf{\Gamma} \in \{0, 1\}^{K_a \times K_a}$ with the (k, k') -th element $\gamma_{k,k'} = 1$ suggesting that the k -th channel belongs to the k' -th group. There is exactly one nonzero element within each row and each column of $\mathbf{\Gamma}$. Then, with the assignment result, each group center is updated as the mean of its constituent channel vectors. The algorithm iteration stops when the maximum number of iterations is reached or there are no further changes in center locations. The algorithm complexity is dominated by the Hungarian algorithm ($\mathcal{O}(K_a^3)$) and yields the order of $\mathcal{O}(SK_a^3)$.

4.2 Codeword Collision Resolution

Codeword collision happens when more than one user chooses to send the same codeword at the same time. The corresponding channel to the reused codeword is the sum of all competitive user channels. The key idea to resolve codeword collision is to identify contaminated channels: they usually have a longer sum distance from all group center points. With a carefully designed data split profile, the probability that more than two users choose to send the same codeword tends to be zero. Therefore, if $K_s < K_a$ channels are determined active, we recognize $K_a - K_s$ channels having the largest aggregated distance to all center points as contaminated channels,

and the corresponding distance row vectors are dublicately added to the original distance matrix to complete a square matrix as algorithm input. However, after data partitioning, the center points of groups involving contaminated channels cannot be updated directly. Luckily, the original center points containing representative user channel statistics can be used to eliminate interfering channels. Specifically, a unique angular domain channel support pattern is extracted from the corresponding center by selecting entries $\{c_m, m \in \mathcal{M}\}$ that concentrate most (e. g., 95%) of the energy, i. e., the elements in \mathcal{M} are chosen as $\sum_{\mathcal{M}} |c_m|^2 > 0.95 \|\mathbf{c}\|_2^2$. Then, only elements within the set $\{\mathbf{g}_{k,m}, m \in \mathcal{M}\}$ are taken for center location update. The complete algorithmic iteration steps are summarized in Algorithm 2.

Algorithm 2. Slot-balanced K -means for message stitching

Input: $\{\mathbf{g}_k^s: k \in [|\mathcal{X}_s|], s \in [S]\}, T_c$

Initialize: $\mathbf{C}(0, S) = [\mathbf{c}_1(0, S), \dots, \mathbf{c}_{K_s}(0, S)]$

for $t = 1, \dots, T_c$ **do**

Set $\mathbf{C}(t, 0) = \mathbf{C}(t - 1, S)$

for $s = 1, \dots, S$ **do**

Compute \mathbf{D} with elements $d_{k,k'} = \|\mathbf{g}_k^s - \mathbf{c}_{k'}\|$

if $K_s < K_a$ **then**

Add $K_a - K_s$ rows with the largest sum of elements

end if

Execute Hungarian algorithm with input \mathbf{D} and output $\mathbf{\Gamma}$

if $K_s < K_a$ **then**

$\forall k': \mathbf{c}_{k'}(t, s) = \frac{1}{s} \left[(s - 1) \mathbf{c}_{k'}(t, s - 1) + \sum_{k=1}^{K_s} \gamma_{k,k'} \mathbf{g}_k^s \right]$

else

$\forall k': \mathbf{c}_{k'}(t, s) = \frac{1}{s} \left[(s - 1) \mathbf{c}_{k'}(t, s - 1) + \sum_{k=1}^{K_s} \gamma_{k,k'} \text{diag}(v_1, \dots, v_M) \mathbf{g}_k^s \right]$, where $v_m \in \{0, 1\}$ is nonzero

when $m \in \mathcal{M}(t, s - 1)$

end if

end for

if $\mathbf{C}(t, S) = \mathbf{C}(t - 1, S)$, **stop**

end for

Output: Partitioning of the data set

5 Simulation Results

In simulations, we consider a URA system with $K_a = 50$ active users randomly and uniformly located in a cell with the radius of 1 km. User channels are generated based on Eq. (1), where $L=4$. Each active user sends a 100 bit message which is divided into $S = 10$ fragments of length $J = 10$. Accordingly, the common codebook $\hat{\mathbf{A}}$ for data transmission is an i. i. d. Gaussian matrix of size 100×2^{10} . The CFO parameter ω is chosen uniformly from the range $(-0.0133, 0.0133)^{[16]}$.

We first examine the proposed MC-PBiGAMP for JADCE under CFO. As the stopping criteria for the iterative algorithm,

we set $T_{\max} = 100$, $T_{\text{mc}} = 20$, and the precision tolerance $\tau = 10^{-4}$. Since we focus on whether active codewords are properly determined, the misdetection rate is used as the AD performance metric, i.e.,

$$P_m = \frac{|\mathcal{A} \setminus \mathcal{X}|}{|\mathcal{A}|}, \quad (29)$$

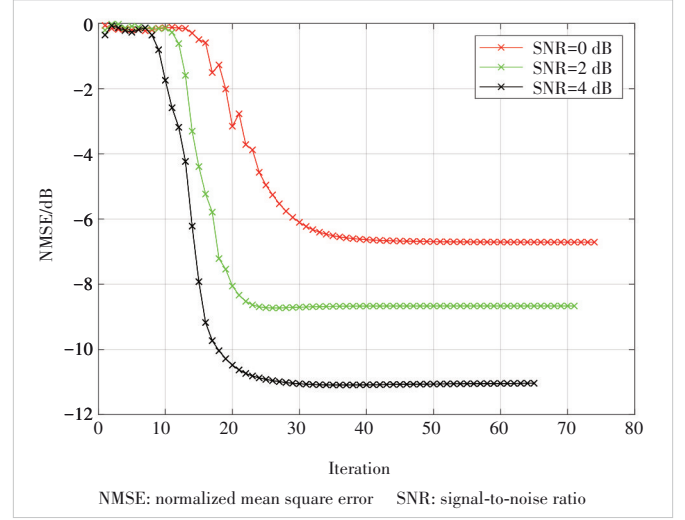
where \mathcal{A} is the set of indexes of active codewords. The algorithm in the aspect of CE is assessed by the normalized mean square error (NMSE) of the recovered active channels, i.e., $\text{NMSE} = \|\bar{\mathbf{X}} - \mathbf{X}_a\|_F^2 / \|\bar{\mathbf{X}}\|_F^2$, where $\bar{\mathbf{X}}$ is the original channel matrix arranged according to the indexes in Eq. (28), and \mathbf{X}_a is the estimated active channel matrix. The NMSE performance of MC-PBiGAMP in each iteration is exhibited in Fig. 2. We observe that the proposed algorithm converges around 65–74 iteration rounds under different signal-to-noise ratios (SNRs).

For comparison, we appeal to the method in Ref. [16]. To deal with the influence of CFO, the discrete CFO parameters $[\omega_1, \dots, \omega_R]$ with $R = 9$ are uniformly sampled from the possible range. JADCE is then performed using the MMV-GAMP algorithm^[14] with the measurement matrix constructed by expanding the original one with these sampled frequency offsets. We also investigate the PBiGAMP algorithm^[22] with no support structure for JADCE. The JADCE performance of the aforementioned methods versus the SNR or the number of measurements N_s is depicted in Fig. 3. The proposed MC-PBiGAMP algorithm outperforms the original PBiGAMP algorithm as we take into account the correlation between adjacent angular domain channel elements by the MC support model. Although MC-PBiGAMP with respect to the AD performance is about the same as MMV-GAMP in Ref. [16], the advantage lies in that it only needs to handle a CFO estimation problem of scale $2^J \times N_s \times M$ compared with the latter of scale $D \times 2^J \times N_s \times M$. It is indicated in Fig. 3(c) that the misdetection rates of both algorithms decrease significantly when $N_s > K_a$. This coincides with the scaling law of AMP that requires measurements to reliably identify a subset of K_a active codewords among a set of size 2^J scales as $N_s = \mathcal{O}\left(K_a \log \frac{2^J}{K_a}\right)$, i.e., N_s is almost linearly with K_a .

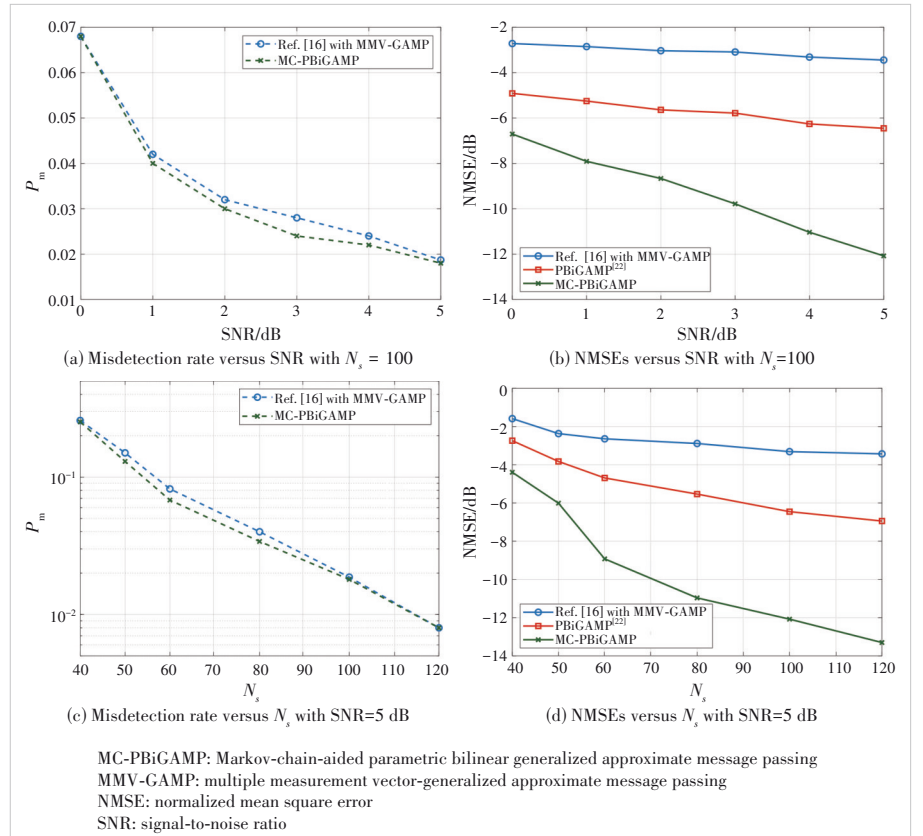
The error rate of URA transmission is defined as the average per user probability of error (PUPE)^[8], i.e.,

$$\text{PUPE} = \mathbb{E} \left\{ \frac{|\mathcal{L} \setminus \{m(k), k \in \mathcal{K}_a\}|}{|\mathcal{L}|} \right\}, \quad (30)$$

where $m(k)$ is the message of the k -th active user in the set \mathcal{K}_a , and \mathcal{L} is the recovered message list. Fig. 4 presents the error rates of uncoupled compressed sensing (UCS) schemes le-



▲ Figure 2. NMSEs versus the iteration number under different SNRs with $M=32$, $N_s=100$, and $K_a=50$



▲ Figure 3. Joint AD and CE (JADCE) performance of various algorithms with $M=32$, $K_a=50$

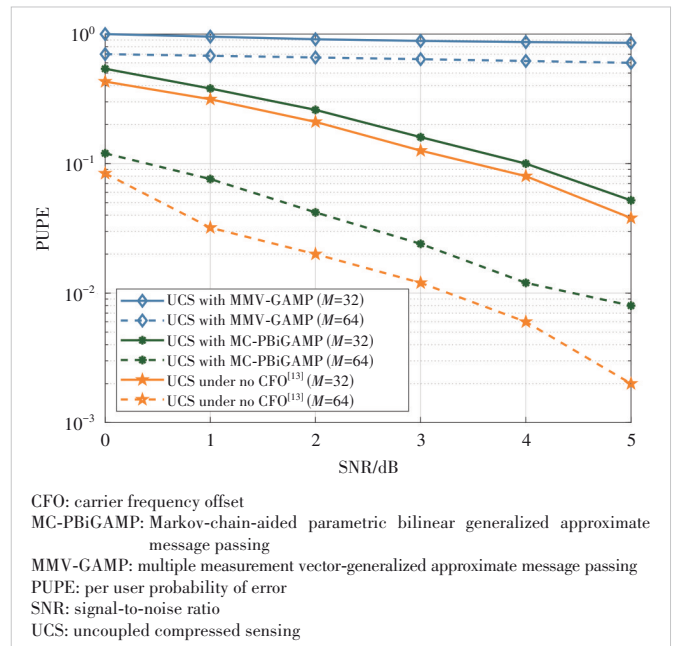
veraging different algorithms for JADCE under CFO. As revealed in Fig. 4, the proposed UCS scheme with PBiGAMP reaches the best system performance with spectral efficiency $\Psi = BK_a/ SN_s = 5$ bit/s per channel use. Fig. 4 also indicates that PUPE improves significantly when the number of receiving antennas is increased. It is due to the higher resolution offered by massive antennas, which not only makes the CS paradigm sparser but also provides more dimensional information for measuring channel similarity. We also draw in Fig. 4 the error rate of URA under no CFO using the method of Ref. [13] as the baseline. It is shown that the proposed approach under CFO pays 0.4 dB (for $M = 32$) to 1.2 dB (for $M = 64$) in terms of SNR to achieve the target PUPE = 0.05 compared with the benchmark.

6 Conclusions

This paper investigates MIMO URA countering the influence of CFO. We formulate URA under CFO as a CS recovery problem with a bilinear graphic structure. The MC-PBiGAMP algorithm is first employed for JADCE with an MC support structure to model the clustered sparsity of the considered angular domain channel. Then, an uncoupled transmission protocol is adopted to reduce the computational burden, where messages are split into several fragments for slotted transmission and stitched together upon clustering user channels. We show by simulations that the proposed scheme is capable of conducting reliable URA transmission under CFO.

References

- [1] DAWY Z, SAAD W, GHOSH A, et al. Toward massive machine type cellular communications [J]. *IEEE wireless communications*, 2017, 24(1): 120 – 128. DOI: 10.1109/MWC.2016.1500284WC
- [2] WU Y P, GAO X Q, ZHOU S D, et al. Massive access for future wireless communication systems [J]. *IEEE wireless communications*, 2020, 27(4): 148 – 156. DOI: 10.1109/MWC.001.1900494
- [3] SENEL K, LARSSON E G. Grant-free massive MTC-enabled massive MIMO: a compressive sensing approach [J]. *IEEE transactions on communications*, 2018, 66(12): 6164 – 6175. DOI: 10.1109/TCOMM.2018.2866559
- [4] LIU L, YU W. Massive connectivity with massive MIMO—part I: device activity detection and channel estimation [J]. *IEEE transactions on signal processing*, 2018, 66(11): 2933 – 2946. DOI: 10.1109/TSP.2018.2818082
- [5] KE M L, GAO Z, WU Y P, et al. Compressive sensing-based adaptive active user detection and channel estimation: massive access meets massive MIMO [J]. *IEEE transactions on signal processing*, 2020, 68: 764 – 779. DOI: 10.1109/TSP.2020.2967175
- [6] KE M L, GAO Z, WU Y P, et al. Massive access in cell-free massive MIMO-based Internet of Things: Cloud computing and edge computing paradigms [J]. *IEEE journal on selected areas in communications*, 2021, 39(3): 756 – 772. DOI: 10.1109/JSAC.2020.3018807
- [7] WEI F, CHEN W, WU Y P, et al. Message-passing receiver design for joint channel estimation and data decoding in uplink grant-free SCMA systems [J]. *IEEE transactions on wireless communications*, 2018, 18(1): 167 – 181. DOI: 10.1109/TWC.2018.2878571
- [8] POLYANSKIY Y. A perspective on massive random-access [C]//International Symposium on Information Theory (ISIT). IEEE, 2017: 2523 – 2527. DOI: 10.1109/ISIT.2017.8006984
- [9] AMALLADINNE V K, CHAMBERLAND J F, NARAYANAN K R. A coded



▲ Figure 4. Error probabilities of various unsourced random access (URA) schemes under CFO as a function of SNR with $N_s=100, K_a=50$

- compressed sensing scheme for unsourced multiple access [J]. *IEEE transactions on information theory*, 2020, 66(10): 6509 – 6533. DOI: 10.1109/TIT.2020.3012948
- [10] FENGLER A, HAGHIGHATSHOAR S, JUNG P, et al. Non-Bayesian activity detection, large-scale fading coefficient estimation, and unsourced random access with a massive MIMO receiver [J]. *IEEE transactions on information theory*, 2021, 67(5): 2925 – 2951. DOI: 10.1109/TIT.2021.3065291
 - [11] XIE X Y, WU Y P, GAO J Y, et al. Massive unsourced random access for massive MIMO correlated channels [C]//IEEE Global Communications Conference. IEEE, 2021: 1 – 6. DOI: 10.1109/GLOBECOM42002.2020.9347959
 - [12] SHYIANOV V, BELLILI F, MEZGHANI A, et al. Massive unsourced random access based on uncoupled compressive sensing: another blessing of massive MIMO [J]. *IEEE journal on selected areas in communications*, 2021, 39(3): 820 – 834. DOI: 10.1109/JSAC.2020.3019722
 - [13] XIE X Y, WU Y P. Unsourced random access with a massive MIMO receiver: Exploiting angular domain sparsity [C]//IEEE/CIC International Conference on Communications in China (ICCC). IEEE, 2021: 741 – 745. DOI: 10.1109/ICCC52777.2021.9580441
 - [14] XIE X Y, WU Y P, AN J P, et al. Massive unsourced random access: exploiting angular domain sparsity [J]. *IEEE transactions on communications*, 2022, 70(4): 2480 – 2498. DOI: 10.1109/TCOMM.2022.3153957
 - [15] LI Y, XIA M H, WU Y C. Activity detection for massive connectivity under frequency offsets via first-order algorithms [J]. *IEEE transactions on wireless communications*, 2019, 18(3): 1988 – 2002. DOI: 10.1109/TWC.2019.2901482
 - [16] SUN G L, LI Y N, YI X P, et al. Massive grant-free OFDMA with timing and frequency offsets [J]. *IEEE transactions on wireless communications*, 2022, 21(5): 3365 – 3380. DOI: 10.1109/TWC.2021.3121066
 - [17] BELLILI F, SOHRABI F, YU W. Generalized approximate message passing for massive MIMO mmWave channel estimation with Laplacian prior [J]. *IEEE transactions on communications*, 2019, 67(5): 3205 – 3219. DOI: 10.1109/TCOMM.2019.2892719
 - [18] FENGLER A, JUNG P, CAIRE G. SPARCs for unsourced random access [J]. *IEEE transactions on information theory*, 2021, 67(10): 6894 – 6915. DOI: 10.1109/TIT.2021.3081189
 - [19] DENG W, SIRIBURANON T, MUSA A, et al. A sub-harmonic injection-locked quadrature frequency synthesizer with frequency calibration scheme for millimeter-wave TDD transceivers [J]. *IEEE journal of solid-state circuits*, 2013, 48(7): 1710 – 1720. DOI: 10.1109/JSSC.2013.2253396

- [20] MYERS N J, HEATH R W. Message passing-based joint CFO and channel estimation in mmWave systems with one-bit ADCs [J]. IEEE transactions on wireless communications, 2019, 18(6): 3064 - 3077. DOI: 10.1109/TWC.2019.2909865
- [21] CHEN L, LIU A, YUAN X J. Structured turbo compressed sensing for massive MIMO channel estimation using a Markov prior [J]. IEEE transactions on vehicular technology, 2018, 67(5): 4635 - 4639. DOI: 10.1109/TVT.2017.2787708
- [22] PARKER J T, SCHNITER P. Parametric bilinear generalized approximate message passing [J]. IEEE journal of selected topics in signal processing, 2016, 10(4): 795 - 808. DOI: 10.1109/JSTSP.2016.2539123
- [23] KUHN H W. The Hungarian method for the assignment problem [J]. Naval research logistics, 2005, 52(1): 7 - 21. DOI: 10.1002/nav.20053

Biographies

XIE Xinyu received his BS degree in telecommunication engineering from Xidian University, China in 2019. He is currently working toward a PhD degree in electronic engineering at Shanghai Jiao Tong University, China. His research interests include massive random access and compressed sensing.

WU Yongpeng (yongpeng.wu@sjtu.edu.cn) received his BS degree in telecommunication engineering from Wuhan University, China in July 2007, and PhD degree in communication and signal processing from the National Mobile Communications Research Laboratory, Southeast University, China in 2013. He is currently a tenure-track associate professor with the Department of Electronic Engineering, Shanghai Jiao Tong University, China. His research interests include massive MIMO/MIMO systems, massive machine type communication, physical layer security, and signal processing for wireless communications.

YUAN Zhifeng received his MS degree in signal and information processing from Nanjing University of Post and Telecommunications, China in 2005. From 2004 to 2006, he was mainly engaged in FPGA/SOC ASIC design. He has been a member of the Wireless Technology Advance Research Department, ZTE Corporation since 2006 and has been responsible for the research of the new multiple access group since 2012. His research interests include wireless communication, MIMO systems, information theory, multiple access, error control coding, adaptive algorithm, and high-speed VLSI design.

MA Yihua received his BE degree from Southeast University, China in 2015 and MS degree from Peking University, China in 2018. He is now a pre-research expert engineer in the Department of Wireless Algorithm, ZTE Corporation. His main research interests include mMTC, grant-free transmissions, NOMA, and joint communication and sensing. In these areas, he has published and applied more than 10 papers and 20 patents.